Catalytic Activity of MoO_3 and V_2O_5 Highly Dispersed on TiO_2 for Oxidation Reactions

Takehiko Ono,* Yoshiro Nakagawa, Hisashi Miyata, and Yutaka Kubokawa
Department of Applied Chemistry, University of Osaka Prefecture, Sakai, Osaka 591
(Received December 3, 1983)

The structure of Mo-Ti oxide catalysts has been investigated by using IR and XRD techniques. At a low Mo content, MoO_3 is highly dispersed on TiO_2, an amorphous phase being formed. Simultaneously, a shift of the Mo=O band from 995 cm^{-1} to 950 and 905 cm^{-1} takes place. The maximum rate of the oxidation of C_2H_5OH and C_3H_6 over Mo-Ti-6(atom% of Mo) is attributable to the weakening of the Mo=O bond. The ^{18}O tracer and kinetic studies of the oxidation of C_3H_6 over Mo-Ti and V-Ti oxides suggest that a redox mechanism is applicable, the rate constants of reduction and reoxidation step being determined. The promoter action of TiO_2 support is attributed mainly to the increase in the rate of reduction step.

Previously we have reported that the promoter effect observed with V-Sn and Mo-Sn oxide catalysts in C_3H_6 oxidation arises from the formation of an amorphous material between each component in those composite catalysts.[1-3] It has been also shown that an amorphous phase formed with V-Ti oxides[4] at a low vanadium content is characterized by vanadate dispersed on TiO_2 in a monolayer, its distorted structure bringing about the weakening of V=O bond, *i.e.*, enhancement of the activity for the oxidative dehydrogenation of C_2H_5OH. As regards Mo-Ti oxide catalysts, a number of workers have studied the correlation between the surface structure and the catalytic activity by means of various techniques such as XRD,[5] IR,[5,6,7] XPS,[8] and *etc.*[7,9] Our understanding of this problem, however, is very far from complete.

In this work, the structure of Mo-Ti oxide catalysts have been investigated in a similar manner to that used in the studies of V-Ti oxides,[4] its correlation with the activity for the oxidative dehydrogenation of C_2H_5OH being examined. With V-Sn and V-Mo oxide catalysts, the nature of the oxygen species responsible for C_3H_6 oxidation has been recently discussed on the basis of the results of ^{18}O tracer and kinetic studies.[2] Similar studies have been extended to Mo-Ti as well as V-Ti oxide catalysts, since such studies are expected to provide information on the nature of the active phase of those catalysts.

Experimental

Materials. Mo-Ti oxides were prepared as follows: The slurry containing desired quantities of TiO_2 (p-25, Degussa) and ammonium heptamolybdate was evaporated with constant stirring. The dried product was calcined at 400 °C. MoC_3 was prepared by heating ammonium heptamolybdate at 450 °C. The surface area of the catalysts determined by the BET method were as follows: TiO_2, 45; Mo-Ti-3 (containing Mo in 3 atom%), 43; Mo-Ti-6, 41; Mo-Ti-24, 30; Mo-Ti-55, 15; MoO_3, 2 m^2/g. The V-Ti oxide catalysts used were the same as those in the previous paper.[4] $^{18}O_2$(99.1 atom%) was obtained from B.O.C. Limited (U. K.).

Apparatus and Procedures. The catalytic oxidation of C_3H_6 and C_2H_5OH was carried out in a closed circulation system (*ca.* 290 cm^3). The reaction products such as CH_2=CHCHO, CO, CO_2, CH_3CHO, and CH_3COCH_3, were analyzed by gas chromatography. The ^{18}O% in the reaction products were determined with a Hitachi RMU-6E mass spectrometer using the following ionization voltage: 80 eV for CO and CO_2, 15.5 eV for H_2O, and 15 eV for CH_2=CHCHO. X-Ray diffraction patterns (XRD) of the catalysts were obtained on both Rigaku Denki D-3F and RAD-rA diffractometers using Cu $K\alpha$ radiation with a Ni filter. With RAD-rA, the goniometer moter system and the signal were interfaced with a versatile data-aquisition system. The RAD-rA diffractometer can detect a small amount of crystalline MoO_3 at a lower Mo content. IR spectra of Mo-Ti oxides were recorded on a Hitachi EPI-G2 infrared spectrometer.

Results and Discussion

Structure of Mo-Ti Oxides. XRD patterns of Mo-Ti oxides showed only lines due to MoO_3 and TiO_2 phases. Figure 1 shows the XRD patterns of MoO_3 phase in Mo-Ti-3 and -6 as well as in their corresponding mechanical mixtures of pure MoO_3 and TiO_2. The intensities of the diffraction lines due to MoO_3 in the Mo-Ti catalysts are much smaller than those of the corresponding mixtures. With Mo-Ti-3, about 100% of the Mo oxide is present as an amorhous phase and

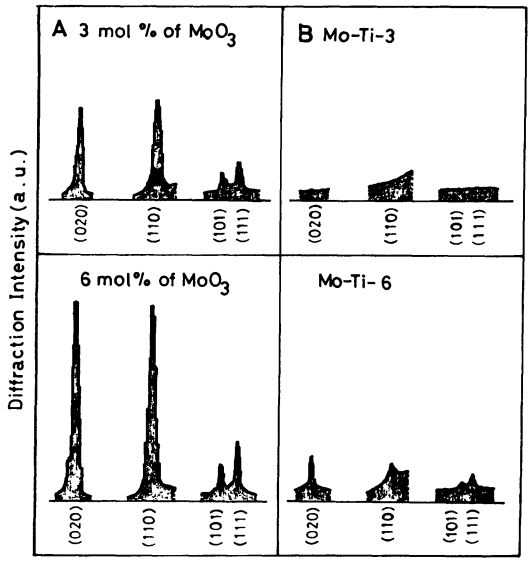

Fig. 1. X-Ray diffraction intensities of Mo-Ti oxides. (A) Mechanical mixtures of molybdenum and titanium oxides; (B) Mo-Ti oxide catalysts. (*hkl*) denote the crystal planes of MoO_3. Each diffraction line was integrated at 0.05° intervals of diffraction angle for 20 s.

with Mo-Ti-6 about 80—90%. Figure 2 shows the average intensities with Mo-Ti-24 and -55 together with the corresponding values for Mo-Ti-3 and -6. With Mo-Ti-24 and -55 catalysts MoO_3 crystals are somewhat oriented in a particular direction. As shown in Fig. 2, most of MoO_3 is amorphous at a low Mo content, its crystallinity increasing at a higher Mo content.

The IR spectra of Mo-Ti oxides containing more than 24 atom% of Mo show sharp bands at 995 and 885 cm^{-1} due to MoO_3(Fig. 3c, d). With Mo-Ti-3 and -6, these band are scarcely observed (Fig. 3 a, b). As has been done in the case of V-Ti oxides,[4], the TiO_2 disk, the weight of which corresponds to the TiO_2 content in the Mo-Ti oxides, was placed in the reference beam in order to offset the absorption due to TiO_2. As shown in Fig. 3e, f, the new bands at 950 and

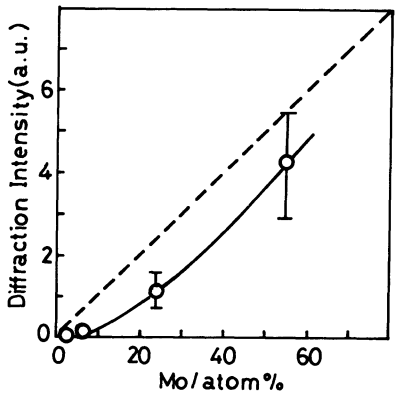

Fig. 2. X-Ray diffraction intensities of MoO_3 in the TiO_2-MoO_3 mixtures (dotted line) and in Mo-Ti catalysts (solid line) as a function of Mo content.

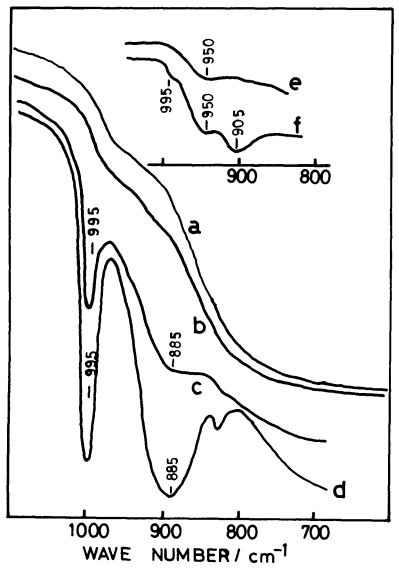

Fig. 3. IR spectra of Mo-Ti oxides. (a) Mo-Ti-3; (b) Mo-Ti-6; (c) Mo-Ti-24; (d) Mo-Ti-55; (e) and (f) the absorption due to TiO_2 were subtracted from (a) and (b) by placing the disk in the reference beam, respectively. 75 mg of KBr disk in 1 wt% of sample was used.

905 cm^{-1} appear with Mo-Ti-3 and -6 catalysts.

According to a number of workers,[10-13] the Raman spectra of various molybdenum-oxygen polyanions show two or three bands in each frequency region of about ≈200, 310—370, 500—600, 700—850, and 900—1000 cm^{-1}; the bands in the last region have been assigned to the stretching vibration of terminal Mo=O groups.[14] From these results the bands at 950—900 cm^{-1} observed with Mo-Al oxide catalysts have been attributed to the surface molybdate on alumina by Jezirowski *et al.*[14] A similar assignment has been made with the bands around 970 cm^{-1} for Mo-Si oxide catalysts.[15,16] Thus the two bands at 950 and 905 cm^{-1} seem to be assigned to terminal Mo=O stretches of the surface molybdate on TiO_2.

The bands at 995(s), 885(s), 820(w), 600(s), and 480(w) cm^{-1} are observed with IR spectra of crystalline MoO_3, while the bands at 995(m), 821(s), 668(w), and 494(vw) cm^{-1} appear in its Raman spectra.[16,17] The band at 995 cm^{-1} appears in both spectra, while the band at 885 cm^{-1} in the IR alone, suggesting that the vibrational modes attributable to both bands appear to be different from each other. Since it has been established that the band at 995 cm^{-1} is assigned to the Mo=O stretching vibration, some other assignment should be made for the band at 885 cm^{-1}.

From these facts it is concluded that with Mo-Ti oxide catalysts at a low Mo content, MoO_3 is highly dispersed on TiO_2 and present as an amorphous state which is characterized by the surface molybdate on TiO_2. Its formation results in distortion of the structure, *i.e.*, shift of the Mo=O band from 995 cm^{-1} to 950 and 905 cm^{-1}. A similar conclusion has been drawn for V-Ti oxides where formation of surface vanadate on TiO_2 brings about the shift of the V=O band from 1020 to 980 cm^{-1}.[4]

Oxydative Dehydrogenation of C_2H_5OH over Mo-Ti Catalysts. Figure 4 shows the rate of oxydative dehydrogenation of C_2H_5OH and the selectivity towards CH_3CHO formation as a function of Mo content at 180 °C. The major product is CH_3CHO, the remainder being $CH_3COOC_2H_5$ and trace of CO_2. The rate passes through a maximum around Mo-Ti-6. The maximum rate is *ca.* 4 times and 30—40 times larger than that at MoO_3 and TiO_2, respectively. There is no marked difference between the rates of oxidation in the presence and absence of oxygen (Fig. 4). Furthermore, essentially the same selectivities towards CH_3CHO formation is obtained with both oxidations. This suggests that lattice oxygen is responsible for the oxydative dehydrogenation over Mo-Ti oxide catalysts.

The rate measurements at various O_2 and C_2H_5OH pressures showed that with MoO_3 the order of the reaction is −0.5 in C_2H_5OH and zero in O_2, while with Mo-Ti-3 and Mo-Ti-6 the corresponding order is zero and 0.2—0.3, respectively. This suggests that the kinetics observed with MoO_3 is in disagreement with what is expected from a redox mechanism; the negative order in C_2H_5OH might arise from its strong adsorption.

As described above, with Mo-Ti-3 and -6 almost the whole MoO_3 is present as the amorphous surface species, while with Mo-Ti oxides containing more than

above 20 atom% of Mo, a considerable fraction MoO_3 consists of crystalline MoO_3.

Accordingly, in the region of a low Mo content, the activity of Mo-Ti oxides for the dehydrogenation of C_2H_5OH increases with increasing Mo content owing to the increase in the concentration of amorphous surface species. In the region of a high Mo content, the increase in the Mo content will cause an increase in the fraction of crystalline MoO_3 which is less active than the surface molybdate species. Thus, it is explicable that the oxidation activity passes through a maximum around 6 atom% of Mo. Such a feature is the same as that with V-Ti oxide catalysts as reported previously.[4]

C_3H_6 Oxidation over Mo-Ti and V-Ti Catalysts. Figure 5 shows the rates of C_3H_6 oxidation and the product selectivities as a function of Mo content at 400 °C. The rate of oxidation passes through a maximum around Mo-Ti-6. Almost the same distribution of the products is obtained in the whole range of the Mo content, *i.e.*, the selectivity towards CH_2=CHCHO formation is 25—30%, the remainder being CO, CO_2, and traces of CH_3COCH_3. With TiO_2, there is no formation of CH_2=CHCHO. With MoO_3 and Mo-Ti-6, essentially the same distribution of the products was obtained with both oxidations in the presence and absence of oxygen.

Similar studies have been extended to V-Ti oxide catalysts. The rate of oxidation at 320 °C also passed through a maximum around V-Ti-10 (atom% of V) catalyst. The selectivity towards CH_2=CHCHO formation decreased with decreasing vanadium content from 15—20% for V_2O_5 to 2—3% for V-Ti-10, the remainder being CO and CO_2. No formation of CH_2=CHCHO was observed with TiO_2. The rate of oxidation over V-Ti-10 is *ca.* 4 times higher than that over V_2O_5 and *ca.* 60 times than over TiO_2.

The dependence of the rate of oxidation upon O_2 and C_3H_6 pressure has been investigated with Mo-Ti as well as V-Ti oxides. As shown in Fig. 6, with increasing O_2 pressure, the rate of oxidation increases markedly for Mo-Ti-6 and V-Ti-10, while a slight increase in the rate is observed for MoO_3 and V_2O_5. There was no marked difference in the dependence of the rate of oxidation on C_3H_6 pressure over V-Ti-10 and V_2O_5. The situa-

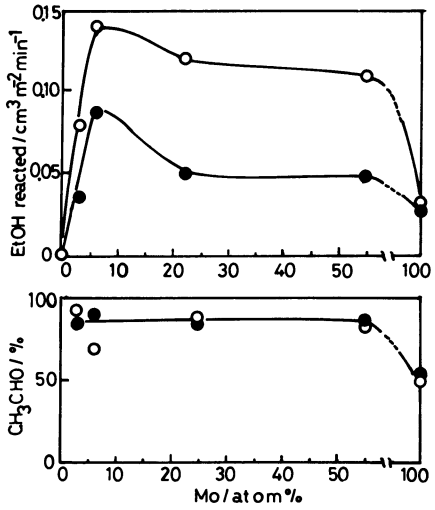

Fig. 4. Oxydative dehydrogenation of C_2H_5OH over Mo-Ti oxide catalysts at 180°C. (○) $P(C_2H_5OH)$= 6 Torr and $P(O_2)$=18 Torr; (●) $P(C_2H_5OH)$=6 Torr and $P(N_2)$=20 Torr; 1 Torr=133.3 Pa.

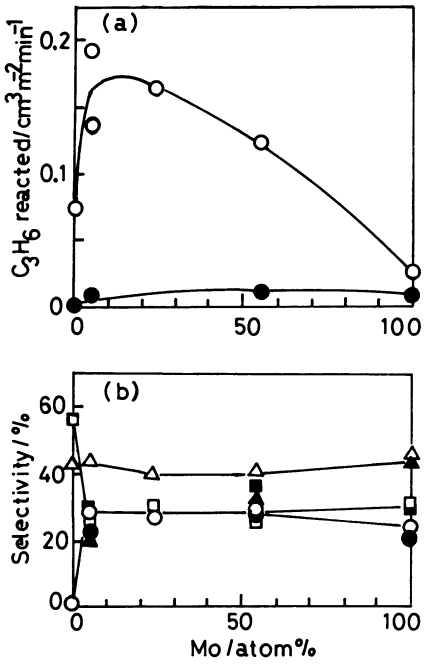

Fig. 5. Rates and product selectivities in C_3H_6 oxidation as a function of Mo content at 400°C. (a) ○ $P(C_3H_6)$=23 Torr and $P(O_2)$=25 Torr, ● $P(C_3H_6)$= 23 Torr. (b) ○●, CH_2=CHCHO; □■ CO_2; △▲ CO. Solid symbols denote the results in the absence of gaseous oxygen.

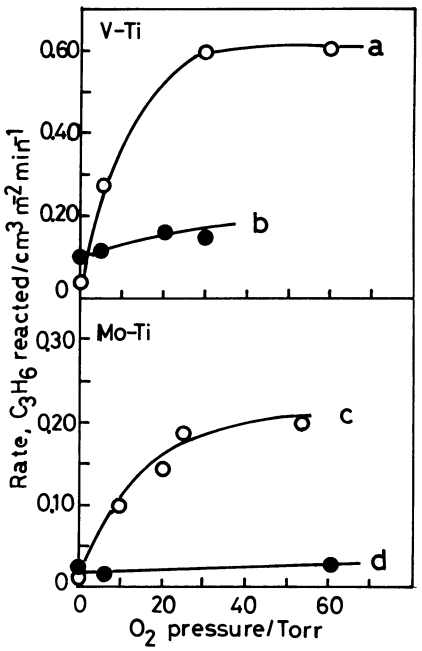

Fig. 6. Rates of C_3H_6 oxidation as a function of oxygen pressure. (a) and (b) are for V-Ti-10 and V_2O_5, respectively, at 320°C and (c) and (d) for Mo-Ti-6 and MoO_3 at 400°C. $P(C_3H_6)$=23 Torr.

tion, however, was different with Mo-Ti-6 and MoO_3, *i.e.*, the order in C_3H_6 was *ca.* 0.3 for Mo-Ti-6 but *ca.* 0.9 for MoO_3.

^{18}O Tracer and Kinetic Studies of C_3H_6 Oxidation. A large dependence of the rate of C_3H_6 oxidation on oxygen pressure observed with Mo-Ti-6 and V-Ti-10 suggests the possibility of participation of adsorbed oxygen in the oxidation. In order to obtain information on the nature of oxygen species responsible for the C_3H_6 oxidation over those catalysts, the oxidation of C_3H_6 has been investigated using $^{18}O_2$ tracer (99 atom%) with the results shown in Table 1 and Fig. 7. Little or no change in the ^{18}O content of the oxygen occurred during the reaction. According to the work of Blanchard *et al.*,[18] the exchange of oxygen through CO_2 appears to be negligible under the present experimental conditions.

In spite of the use of 99% of $^{18}O_2$, the ^{18}O content in the products at the initial stages of the reaction ranges from 20 to 30% for Mo-Ti-6 and MoO_3 and 15 to 20% for V-Ti-10 and V_2O_5. This indicates that the lattice oxygen(^{16}O) is responsible for the oxidation over both oxide catalysts. As has been done by Keulks *et al.*,[19] assuming uniform distribution of the incorporated ^{18}O among the sublayer of the oxides and the number of oxygen atoms in unit area (20 μmol/m^2), the extent of participation has been determined as follows: V_2O_5(*ca.* 10 layers)>V-Ti-10(*ca.* 5 layers)>V-Ti-2(*ca.* 1 layer) and Mo-Ti-6(*ca.* 5 layers)=MoO_3(*ca.* 5 layers).

As described previously,[2] even in the case where the surface anion vacancies are not refilled from gaseous oxygen, the following equation based on a simple redox mechanism holds, as far as the diffusion of the oxide ion is rapid as compared to the surface reduction;[2]

$$k_1P(C_3H_6)\theta = k_2P(O_2)^{0.5}(1-\theta), \quad (1)$$

where k_1 is the rate constant for reduction step and k_2 for reoxidation step. θ and $1-\theta$ refer to the surface oxide ions and anion vacancies, respectively, which corresponds to the surface Mo=O species and anion vacancies formed by oxygen removed from it, respectively, in view

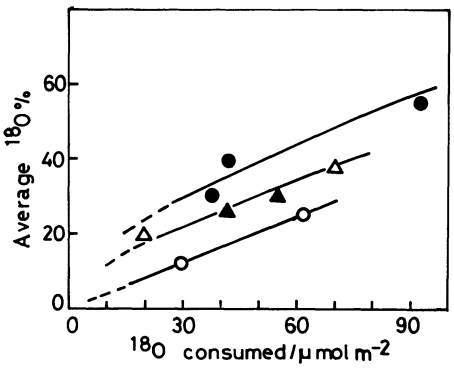

Fig. 7. Average ^{18}O%[a] in the products *vs.* amount of ^{18}O consumed[b] in C_3H_6 oxidation. V-Ti-10(●) and V_2O_5(○) at 320°C, Mo-Ti-6(▲) and MoO_3 (△) at 400°C. a),b) See Table 1.

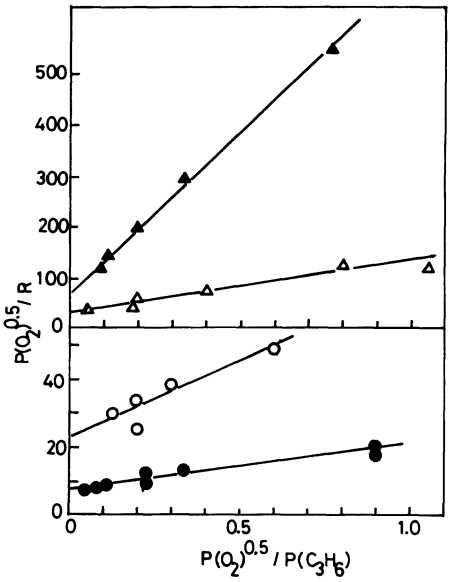

Fig. 8. Plots of $P(O_2)^{0.5}/R$ *vs.* $P(O_2)^{0.5}/P(C_3H_6)$ for MoO_3(▲), Mo-Ti-6(○), V_2O_5(△), and V-Ti-10 (●).
Experimental conditions are the same as in Fig. 5 for Mo-Ti oxides and in Fig. 6 for V-Ti oxides, respectively. R denotes the rate of C_3H_6 oxidation.

Table 1. ^{18}O contents in the products of C_3H_6 oxidation over Mo-Ti and V-Ti oxide catalysts

Catalyst	Temp °C	React. time min	Products/μ mol m^{-2} and ^{18}O content/%[a] CO_2	CO	H_2O[b]	CH_2=CHCHO	Total yield[c] μ mol-oxygen atoms m^{-2}	Average[d] ^{18}O %	Lattice oxygen[e] participated layers
Mo-Ti-6	400	3	7.4(24)	7.1(34)	17(—)	3(19)	42	26	*ca.* 5
MoO_3	400	5.5	2.9(19)	4.2(21)	8(—)	0.8(33)	19	20	*ca.* 5
		15	13(34)	13(39)	28(—)	3(50)	70	37	
V-Ti-10	320	0.2	5(28)	9(33)	7(—)	—	26	30	
		0.3	4(36)	13(43)	17(—)	—	41	40	*ca.* 5
		1.0	14(54)	25(59)	38(39)	—	91	50	
V_2O_5	320	1	3.5(12)	7.5(13)	11(11)	0.45(25)	27	13	*ca.* 10
		3	7.5(25)	16(25)	24(20)	0.75(31)	55	25	

a) Values in parentheses. b) Calculated from hydrogen balance. c) These values were nearly the same as that obtained from the amount of $^{18}O_2$ consumed in the oxidation. d) (Total amount of ^{18}O/total amount of oxygen) × 100. e) See Ref. 19. $P(C_3H_6)=23$ Torr, $P(^{18}O_2)=8$ Torr.

Table 2. Values of k_1 and k_2 for Mo-Ti and V-Ti oxide catalysts

Catalyst	Temp/°C	k_1[a]	k_2[b]
MoO_3	400	0.0015	0.015
Mo-Ti-6	400	0.024	0.04
V_2O_5	320	0.01	0.04
V-Ti-10	320	0.08	0.12

a) $cm^3\ Torr^{-1}\ min^{-1}\ m^{-2}$, b) $cm^3\ Torr^{-1/2}\ min^{-1}\ m^{-2}$.

of the importance of the Mo=O species in the oxidation. The following rate equation results:

$$R = \frac{k_1 k_2 P(C_3H_6) P(O_2)^{0.5}}{k_1 P(C_3H_6) + k_2 P(O_2)^{0.5}}. \quad (2)$$

As shown in Fig. 8, the plots of $P(O_2)^{0.5}/R$ *vs.* $P(O_2)^{0.5}/P(C_3H_6)$ is approximately linear, suggeting that this equation is applicable to the results. Table 2 shows the values of k_1 and k_2 thus obtained.

Both k_1 and k_2 values increase on going from MoO_3 to Mo-Ti-6 and from V_2O_5 to V-Ti-10. The increase in the k_1 value is much larger than that for the k_2 value. Thus, the promoter action of TiO_2 in V-Ti and Mo-Ti oxides is attributed mainly to the increase in the rate of reduction step. Such a relative change of k_1 and k_2 is expected from the weakening of the Mo=O bond as described above. Thus, the rate maximum observed with both oxidation (Figs. 4 and 5) are explicable on the same basis. A large dependence of the rate of oxidation on oxygen pressure over Mo-Ti-6 and V-Ti-10 catalysts is also explicable from high values of k_1/k_2, *i.e.*, the high reducibility of surface molybdate or vanadate on TiO_2. The maximum rate of oxidation for Mo-Ti-6 and V-Ti-10 is explicable in a manner similar to that with the oxydative dehydrogenation of C_2H_5OH, *i.e.*, by the change in the concentration of the surface species with the Mo or V content.

Recently a number of workers have investigated the promoter effect observed with V-Ti oxides in the oxidation reaction, making various proposals.[20-24] The results described above indicate that similar mechanisms are involved in the promoter effects with both Mo-Ti and V-Ti oxides; The role of TiO_2 support in those oxide catalysts is to enhance the activity per one site in addition to the increase in the number of active sites. From the results in the present work together with those obtained previously,[4] it might be concluded that the promoter action due to formation of the amorphous phase (a highly dispersed oxide catalyst) is expected for other composite oxide catalysts.

Akimoto *et al.*[6] have reported that both adsorbed molecular oxygen and lattice oxygen participates in the production of maleic anhydride from 1,3-C_4H_6 over Mo-Ti catalysts. In the case of V-Sn oxide catalysts at a low V content, we have also suggested the participation of both adsorbed and lattice oxygens in the oxidation on the basis of the results of ^{18}O tracer as well as kinetic studies.[2] With Mo-Ti and V-Ti oxide catalysts, however, it seems unnecessry to take into account the possibility of adsorbed oxygen, since the dependence of the rate of oxidation on O_2 and C_3H_6 pressure is explicable by the concept that only lattice oxygen participates in the oxidation.

With the C_3H_6 oxidation over Mo-Ti oxide, there is a marked difference between the rates of oxidation in the presence and absence of oxygen. Such a feature is contrast with a slight difference between the both rates for the oxydative dehydrogenation of C_2H_5OH. It should be noted that the number of lattice oxygen atoms consumed on the oxidation of one molecule is 1—2 with C_2H_5OH but 9—10 with C_3H_6, the lattice oxygen producing CO, CO_2, H_2O, and CH_2=CHCHO for C_3H_6 oxidation. Furthermore, the reaction temperature is much higher for the C_3H_6 oxidation. Accordingly, the extent of oxygen removed from the Mo=O species during the reaction is expected to be much smaller for C_2H_5OH dehydrogenation than for the C_3H_6 oxidation. Thus, a small enhancement of the rate of C_2H_5OH dehydrogenation by the presence of oxygen is explicable.

The authors wish to thank Mr. Makoto Sakaguchi for carrying out part of the experiments.

References

1) T. Ono, Y. Nakagawa, and Y. Kubokawa, *Bull. Chem. Soc. Jpn.*, **54**, 343 (1981).
2) T. Ono and Y. Kubokawa, *Bull. Chem. Soc. Jpn.*, **55**, 1748 (1982).
3) T. Ono, T. Ikebata, and Y. Kubokawa, *Bull. Chem. Soc. Jpn.*, **56**, 1284 (1983).
4) Y. Nakagawa, T. Ono, H. Miyata, and Y. Kubokawa, *J. Chem. Soc., Faraday Trans. 1*, **79**, 2929 (1983).
5) K. Yu. Adzhamov, A. K. Senchikhina, T. G. Alkazov, and K. M. Mekhtiev, *Kinet. Catal.*, **16**, 589 (1975).
6) M. Akimoto and E. Echigoya, *J. Catal.*, **29**, 191 (1973).
7) J. Rivasseau, P. Canesson, and M. Blanchard, *J. Phys. Chem.*, **84**, 2972 (1980).
8) K. Tanaka, K. Miyahara, and Ke. Tanaka, *Bull. Chem. Soc. Jpn.*, **54**, 3106 (1981).
9) M. Ai, *Bull. Chem. Soc. Jpn.*, **49**, 1328 (1976).
10) W. P. Griffith and P. J. B. Lesniak, *J. Chem. Soc.*, A, 1066 (1969).
11) J. Fuchs and K. F. Jahr, *Z. Naturforsch.*, B, **23**, 1380 (1968); J. Fuchs and J. Brudgam, *ibid.*, **32**, 853 (1977).
12) K. H. Tytko and B. Schonfeld, *Z. Naturforsch.*, **30**, 471 (1975).
13) R. Mattes, H. Bierbusse, and J. Fuchs., *Z. Anorg. Allg. Chem.*, **385**, 230 (1971).
14) H. Jeziorowskii and H. Knözinger, *J. Phys. Chem.*, **83**, 1166 (1979).
15) S. R. Seyedmouir, S. Abdo, and R. F. Howe, *J. Phys. Chem.*, **86**, 1232 (1982).
16) H. Jeziorowskii, H. Knözinger, P. Grange, and P. Gajardo, *J. Phys. Chem.*, **84**, 1825 (1980).
17) F. R. Brown, Leo E. Makrovsky, and K. H. Rhee, *J. Catal.*, **50**, 162 (1977).
18) M. Blanchard and G. Longuet, *Kinet. Catal.*, **14**, 20 (1973).
19) G. W. Keulks and L. D. Krenzke, *Proc. 6th. Int. Congr. Catal.*, London, 1976, Vol. 2, p. 806; L. D. Krenzke and G. W. Keulks, *J. Catal.*, **61**, 316 (1980).
20) D. J. Cole, C. F. Cullis, and D. J. Hucknall, *J. Chem. Soc., Faraday Trans. 1*, **72**, 2185 (1976).
21) Y. Murakami, M. Inomata, A. Miyamoto, and K. Mori, *Proc. 7th Int. Congr. Catal.*, Tokyo, 1980, P. 1344; A. Miyamoto, Y. Yamazaki, M. Inomata, and Y. Murakami, *J. Phys. Chem.*,

85, 2366, 2372 (1981); M. Inomata, K. Mori, A. Miyamoto, T. Ui, and Y. Murakami, *ibid.*, **87**, 754 (1983).
22) G. C. Bond and K. Buckeman, *Discuss. Faraday Soc.*, **1982**, 235.
23) A. Andersson, *J. Catal.*, **76**, 144 (1982).
24) M. Akimoto, M. Usami, and E. Echigoya, *Bull. Chem. Soc. Jpn.*, **51**, 2195 (1978).